PCCP

Dynamic Article Links ►

Cite this: DOI: 10.1039/c0xx00000x

www.rsc.org/pcp

PAPER

Interaction of Naphthalene Derivatives with Lipid in Membrane Studied by ^{1}H-Nuclear Overhauser Effect and Molecular Dynamics Simulation

Megumi Shintani,[a] Yushi Matsuo,[a] Shun Sakuraba[a] and Nubuyuki Matubayasi [*ab]

Received (in XXX, XXX) Xth XXXXXXXXX 20XX, Accepted Xth XXXXXXXXX 20XX

DOI: 10.1039/b000000x

The location, orientation, and dynamics of hydrophobic small molecule in lipid membrane are studied through combined use of the solution-state ^{1}H-NMR and MD simulation. 1-Naphthol and 1-methylnaphthalene were adopted as the small molecule with or without hydrophilic group. The nuclear Overhauser effect (NOE) measurement was performed for large unilamellar vesicle (100 nm in diameter) composed of dimyristoylphosphatidylcholine (DMPC) and the naphthalene derivative. The transient NOE-SE (spin echo) scheme previously reported (*J. Phys. Chem. B*, 2011, **115**, 9106-9115) was employed to quantitatively determine the NOE cross relaxation rate constant between DMPC and the naphthalene derivative. The observed NOE shows that both the naphthalene derivatives distribute over wide domain across the normal of the essentially planar membrane ranging from the hydrophobic core to the hydrophilic headgroup. The experimental NOE information was further refined in combination with the analysis of time correlation functions in MD simulation. It was found that 1-naphthol exhibits slight preference of its OH group pointing toward the hydrophilic domain of membrane and that no definite preference can be concluded for the orientation of 1-methylnaphthalene. When 1-naphthol and 1-methylnaphthalene are compared, the NOE is the stronger for 1-naphthol due to the restricted motion by the OH group. The slowdown of the 1-naphthol motion is also evidenced by the ^{1}H spectral line width.

1. Introduction

The interaction between small molecule and phospholipid membrane is of importance in determining biological and physiological functions of biomembrane. Medicine and toxin are typically smaller than lipids and regulate biological functions through binding with membrane. Membrane fluidity is further shown to be strongly affected by the presence of cholesterol[1-10] and the permeability of water.[11-14] Membrane functions are determined by cooperation and/or competition of a variety of intra- and intermolecular interaction components. It is thus desired to investigate the interaction between small molecules and phospholipids composing biomembranes at atomic resolution.

Small molecules can permeate a bilayer membrane by the simple diffusion without channels. The permeation process is controlled by the intermolecular interaction between small molecules and phospholipids. Highly polar molecules can hardly pass through the hydrophobic core of the lipid membrane, and nonpolar molecules are expected to stay in the hydrophobic core at high probability. The interplay between hydrophilicity and hydrophobicity is a key to understanding the membrane permeation of small molecules.

[a] *Institute for Chemical Research, Kyoto University, Uji, Kyoto 611-0011, Japan E-mail: nobuyuki@scl.kyoto-u.ac.jp*

[b] *Japan Science and Technology Agency (JST), CREST, Kawaguchi, Saitama 332-0012, Japan*

In this paper, we discuss the location, orientation, and dynamics of small molecules in phospholipid membrane at atomic resolution by using NMR and molecular dynamics (MD) simulation. To conduct a contrasted variation of the substituent in small molecule, we adopt two naphthalene derivatives as small molecules added to dimyristoylphosphatidylcholine (DMPC): 1-naphthol and 1-methylnaphthalene. The molecular structures and the proton numberings are shown in Figure 1. Both of the two have the common building block of aromatic naphthalene ring. The difference is the polar hydroxyl group and the hydrophobic methyl group. The two naphthalene derivatives are chosen due to their simplicity of chemical structure. Their intermolecular interactions are mainly hydrophobic, and the extent of hydrophilicity/hydrophobicity is locally modified. This is helpful

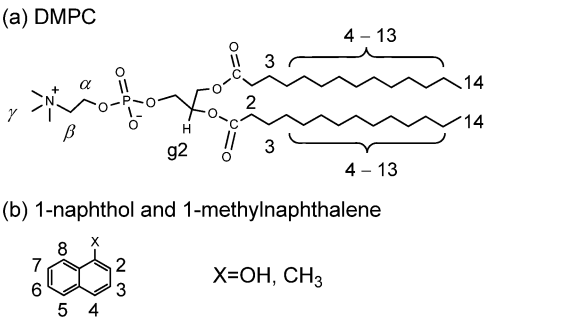

Figure 1. Molecular structures of (a) DMPC and (b) naphthalene derivatives.

to separate the contributions of a variety of interaction components and to discuss the difference in the binding of the small hydrophobic molecules with and without hydrophilic group. In addition, there is a technical advantage that the chemical shifts are well separated from those of lipid and that the asymmetric structures allow the discussion of orientational preference.

The interaction of small molecule with lipid membrane has been well studied by molecular simulation.[9, 15-23] It is found that even a hydrophobic solute is not always localized in the hydrophobic core of membrane and is typically observed to distribute over wide domains from the core to hydrophilic headgroup. Experimental information has been accumulated for somewhat large molecules with varieties of functional groups. Fluorescence and EPR experiments[24] have been done using specially designed probe molecule, and neutron scattering studies have been performed for biologically relevant molecules such as cholesterol[3, 9] and vitamin E[25]. NMR studies have been mainly conducted for multilamellar vesicles at solid state for a diverse set of functional molecules.[5, 6, 13-15, 26-35] The present work focuses on the unilamellar vesicle at solution state. The membrane can be prepared with uniform curvature and the inter-membrane interaction is virtually absent. In this sense, the unilamellar state in solution is suitable as a reference for studying the interaction of lipid membrane with a molecule bound to it. The site-specific information is then important, and the measurement of nuclear Overhauser effect (NOE) is useful to obtain direct information on the internuclear distance and the correlation time between a selected pair of protons.[36-39]

The difficulty of the solution-state ^{1}H-NMR of lipid membrane is that the signals of large vesicles are usually broadened and overlapped significantly. The NMR study of intermolecular correlation in model membranes has thus been restricted to micelle and small vesicles.[40-45] In particular, the conventional NOE measurement is hard to give quantitative information for essentially planar membrane system. In a previous work, we employed a solution-state ^{1}H-NOE sequence through combination with the spin-echo (SE) sequence (transient NOE-SE method).[46] This method suppresses the broad components in spectra of large vesicles and makes possible the quantitative analysis of NOE. In the present work, the NOE analysis of small molecules and lipids is performed at atomic level by utilizing the transient NOE-SE method.

The NOE cross relaxation rate constant reflects both the internuclear distance and correlation time. The separation of the NOE into the distance and time information typically needs an approximation of fixed correlation time or fixed distance.[37] In protein-structure determination, the approximation of fixed correlation time is commonly employed.[39] Our previous work on lipid membrane showed, on the other hand, that the correlation time varies over orders of magnitude for the NOE between lipid sites. In this work, we carry out MD simulation of the planar DMPC bilayer containing the naphthalene derivative and demonstrate that the intermolecular distance between lipid and small molecule governs the NOE between them. The location and orientation of the naphthalene derivative obtained from the experimental NOE are then refined by utilizing the MD correlation time in a semi-quantitative manner. We also use MD simulation to validate the experimental setup. We show that the high concentration of small molecule used in experiment to achieve good S/N does not affect the static and dynamic properties of small molecule in the lipid membrane.

2. Methods

2.1 Experimental Procedures

Lipid bilayer vesicle was formed by dimyristoylphosphatidylcholine (DMPC). DMPC with a purity of 99% was purchased from Wako Pure Chemical Industries. 1-Naphthol and 1-methylnaphthalene were obtained from Nacalai. Chloroform (99%) used for vesicle preparation was supplied by Nacalai. Heavy water (D_2O; 99.9% D) was from Euriso-top (Saint Aubin, France). The aqueous solution of 1-naphthol or 1-methylnaphthalene was prepared by stirring its excess amount in D_2O over 1 hour at 40 ºC.

Large unilamellar vesicle (LUV) containing the naphthalene derivative was prepared as follows. DMPC was first dissolved in chloroform, and the solvent was evaporated overnight to form a thin DMPC film. The lipid film was then hydrated with desired amounts of D_2O and the naphthalene derivative. The aqueous suspension was subjected to freeze-thaw method over eight cycles. The LUV of 100 nm in diameter was finally obtained by the extrusion method as described elsewhere[8, 46] using EXTRUDER (Lipex Biomembranes, Inc.). The sample concentrations of DMPC and the naphthalene derivative were determined from the ^{1}H-NMR signal intensities as described in section 3. The DMPC concentration was 20 mM, and that of the naphthalene derivative was observed to be ~8 mM and corresponds to ~40 mol% relative to DMPC.

All the NMR measurements were performed by using a JEOL ECA600 NMR spectrometer with a specially designed diffusion probe HX5GR.[47] The ^{1}H frequency was 600 MHz. The NMR measurements were conducted at 40 ºC, which is above the gel-liquid crystal phase transition temperature of DMPC (23 ºC[48]). The impurity HDO signal contained in solvent D_2O was used as the internal reference for the chemical shift, which was set to 4.59 ppm. To suppress the excess HDO signal, the pulse-field gradient was used.[49]

The signal assignments of the naphthalene derivatives were carried out using COSY and NOESY. Due to the low concentration and the line broadening in D_2O solution and DMPC vesicles, the assignments with the 2D measurements were performed in *n*-octanol solutions. See Appendix A for the signal assignments.

To obtain well-resolved NOE signals of LUVs at solution state, we employ the transient NOE-SE method.[46] In this method, the conventional transient NOE method is combined with the spin-echo (SE) method. The broad signals in LUVs are suppressed by the spin-echo part of the transient NOE-SE sequence and the sharp signals are detected against apparently flat baseline. The details and performance of the transient NOE-SE method are described in ref 46. In the present study, the delay time of the spin echo τ_{SE} was 3 ms, and the field gradient parameters δ and g were 1.1 ms and 1.5 Tm^{-1}, respectively.

The NOE enhancement factor η is determined from

$$\eta(\tau_m) = \frac{I(\tau_m) - I_{SE}}{n_b I_{SE}}, \quad (1)$$

where I_{SE} is the integrated intensity of the reference spectrum with spin echo and without NOE, $I(\tau_m)$ is the integrated intensity of the sample spectrum modified by NOE, and τ_m is the mixing time. n_b is the number of equivalent protons of the irradiated site b within a single molecule; for example, n_b is 9 when the choline methyl proton of DMPC is irradiated. The reason for the division by n_b is described in subsection 2.2. The cross relaxation rate constant σ was determined from η through

$$\eta(\tau_m) = 2\sigma\tau_m . \quad (2)$$

This is the linear approximation, and is ensured by small enough τ_m. At the same time, τ_m is desirable to be large enough to have η with good S/N. A τ_m value of 100 ms was adopted; with this choice of τ_m, the conditions of the high S/N and of the linearity of η against τ_m are both satisfied. In Appendix B, the validation is shown for our choice of τ_m = 100 ms.

2.2 Theoretical Expressions for NOE

The NOE enhancement factor η in eq. 1 is related through eq 2 to the cross relaxation rate constant σ by the initial rate approximation when τ_m is small enough. For a homonuclear system, σ is provided by the spectral density function $j(\omega)$ through

$$\sigma = \frac{1}{24}\{6j(2\omega_0) - j(0)\}, \quad (3)$$

where ω_0 is the Larmor frequency in angular units. The $j(\omega)$ is given by the Fourier transform of the time correlation function $C(t)$ for the dipole-dipole interaction, and $C(t)$ is expressed as

$$C(t) = \xi\left\langle r(0)^{-3} r(t)^{-3} Y_2^0(\Omega(0)) Y_2^0(\Omega(t))\right\rangle, \quad (4)$$

where t is the time, r is the radial distance between the proton pair of interest, $Y_2^0 = (3\cos^2\theta - 1)/2$ is the normalized second-order spherical harmonics, and $\Omega = (\theta, \varphi)$ is the polar angle for the unit vector connecting the two protons of interest in the laboratory reference frame. The constant ξ is $3\mu_0^2\hbar^2\gamma^4/8\pi^2$, where μ_0 is the permeability of vacuum, $\hbar$ is the Planck constant divided by 2π, and γ is the gyromagnetic ratio of proton. The angular bracket indicates the ensemble average over the equivalent proton pairs and the laboratory frame orientation. The correlation time τ_c is defined as

$$\tau_c = \int_0^\infty \frac{C(t)}{C(0)} dt . \quad (5)$$

The $C(0)$ is expressed by

$$C(0) = \frac{1}{5}\xi\left\langle r^{-6}\right\rangle . \quad (6)$$

$\langle r^{-6}\rangle$ in eq 6 is obtained by

$$\left\langle r^{-6}\right\rangle = \int \rho(r) r^{-6} dr \quad (7)$$

and

$$\rho(r) = \frac{1}{N_a n_b}\sum_a\sum_b \left\langle \delta(r_{ab} - r)\right\rangle, \quad (8)$$

where N_a is the number of observed protons of type a in the whole system and n_b is the number of equivalent protons of the irradiated site b in single molecule; for example, N_a is 3 times the number of the observed molecules in the system when the methyl proton is observed, and n_b is 9 when the choline methyl proton of DMPC is irradiated. Due to the division by n_b in eq 8, the integration of $\rho(r)$ over whole r is the same for any pair of observed a and irradiated b. With this normalization, the comparison is quantitatively possible for internuclear distances among different proton pairs. When $C(t)$ is expressed as a sum of exponential functions through

$$C(t) = \frac{1}{5}\xi\left\langle r^{-6}\right\rangle \sum_n A_n \exp\left(-\frac{t}{\tau_n}\right) \quad (9)$$

with $\sum_n A_n = 1$, the cross relaxation rate constant σ is written as

$$\sigma = \frac{\mu_0^2\hbar^2\gamma^4}{160\pi^2}\left\langle r^{-6}\right\rangle K(\omega_0), \quad (10)$$

where $K(\omega_0)$ is given by

$$K(\omega_0) = \left(6\sum_n \frac{A_n\tau_n}{1 + 4\omega_0^2\tau_n^2} - \sum_n A_n\tau_n\right). \quad (11)$$

When $C(t)$ relaxes much faster than $1/\omega_0$ (motional narrowing limit; $1/\omega_0 \gg \tau_c$), $j(2\omega_0)$ is virtually identical to $j(0)$ and

$$K(\omega_0) = 5\tau_c , \quad (12)$$

where τ_c is the correlation time of eq 5. When $C(t)$ relaxes much slower than $1/\omega_0$ (spin diffusion limit; $1/\omega_0 \ll \tau_c$), $j(2\omega_0)$ is negligibly small and

$$K(\omega_0) = -\tau_c . \quad (13)$$

More theoretical background of the NOE cross relaxation is described in refs 39 and 50.

2.3 MD Procedures

MD simulation was performed for the DMPC planar bilayer system containing 1-naphthol or 1-methylnaphthalene. In each of the 1-naphthol and 1-methylnaphthalene systems, two MD simulations were conducted. One corresponds to the experimental set up and was done at 40 mol% concentration of the naphthalene derivative relative to DMPC, and the other was at 10 mol%. The two sets of MD were run to validate our experimental setup that the naphthalene derivative was incorporated at 40 mol% to obtain high S/N signals in NMR measurements. In the MD unit cell, 288 DMPC and 7392 water molecules were located with 115 and 28 naphthalene-derivative molecules, respectively, for the 40 mol% and 10 mol% systems. The all-atom CHARMM force field PARAM27R was used for lipid[51-54], and the TIP3P model was adopted for the water molecule.[55] 1-Methylnaphthalene was modeled with the standard procedure for CHARMM force field parameters.[56] For 1-naphthol, the charges on the general aromatic ring were assigned directly to the naphthalene ring. The charge on the hydroxyl O was taken to be that on the O of phenol, and the H charge in the hydroxyl group was set so that the molecule is neutral in total.[57]

The periodic boundary condition was employed and the unit cell was taken to be rectangular with the x- and y-directions

corresponding to the membrane lateral and the *z*-direction to the normal. The ensemble adopted was the NP_nAT (constant particle numbers, normal pressure, lateral area, and temperature). The pressure and temperature were controlled at 1 bar and 40 ºC, respectively, with the Nosé-Hoover Langevin method at time constants of 5.0 ps.[1, 58, 59] The lateral area of the unit cell was taken from the experimental value and was set to 93.5 Å^2 in the square form.[60] The electrostatic interaction was handled by the particle-mesh Ewald (PME) method with a real-space cutoff of 12 Å, a spline order of 6, a relative tolerance of 10^{-5}, and the reciprocal-space mesh size of 96×96×72.[61] The Lennard-Jones interaction was truncated by applying the switching function, where the switching range is 10–12 Å.[62] The bond lengths involving hydrogen atom were fixed with SHAKE and the water molecule was kept rigid with SETTLE.[63] The equation of motion was integrated with the velocity Verlet algorithm at a time step of 2 fs.[64] All the MD calculations were done using NAMD ver.2.8[65] for 20 ns for both the 40 mol% and 10 mol% systems. It was found that the concentration effect is practically absent, and all the MD results shown in subsection 3.2 are those from the 40 mol% system. The comparison between the 40 mol% and 10 mol% systems is described in Appendix C.

3. Results and Discussion

In the following, DMPC is abbreviated as PC, and its proton site is represented by referring to the character or number in Figure 1. For example, PCγ stands for the choline methyl protons of DMPC. The proton site in the naphthalene derivative is denoted by H followed by the number in Figure 1. For example, H67 means the proton sites of H6 and H7 of the naphthalene derivative when the ^{1}H signals of H6 and H7 cannot be distinguished in the NMR spectra.

The ring proton regions in the ^{1}H-NMR spectra of 1-naphthol and 1-methylnaphthalene in D_2O and DMPC bilayer are shown in Figure 2. In the DMPC system, the concentrations of the naphthalene derivatives determined from the signal intensities of ring protons are ~8 mM. This concentration is higher than the solubility in water (6 mM for 1-naphthol and ~0.1 mM for 1-methylnaphthalene). The peaks in the DMPC bilayer shift upfield (toward low-frequency region) and are broadened, relative to those in the D_2O solution. The sharp signals observed in D_2O at lower-field (high-frequency) region are not seen in the DMPC system. The above shows for the DMPC system that the naphthalene derivatives are bound within DMPC bilayer, not in bulk water.[67] Note that log $P_{o/w}$ is 2.85 and 3.87 for 1-naphthol and 1-methylnaphthalene, respectively, where $P_{o/w}$ is the octanol-water partition coefficient.[68] Both the naphthalene derivatives have the higher affinities with octanol than with water, being consistent with the observation of their bindings into DMPC membrane.

The chemical shifts of DMPC and the naphthalene derivative vary with the binding. In Appendix A, though, we note that the chemical shift is not a clear indicator of the binding site to distinguish the hydrophilic and hydrophobic domains of bilayer. The NOE can be more suitable for identifying the location and orientation of the small molecule in membrane. In the following subsections, the internuclear distance and the correlation time are examined through combined use of NOE experiment and MD simulation.

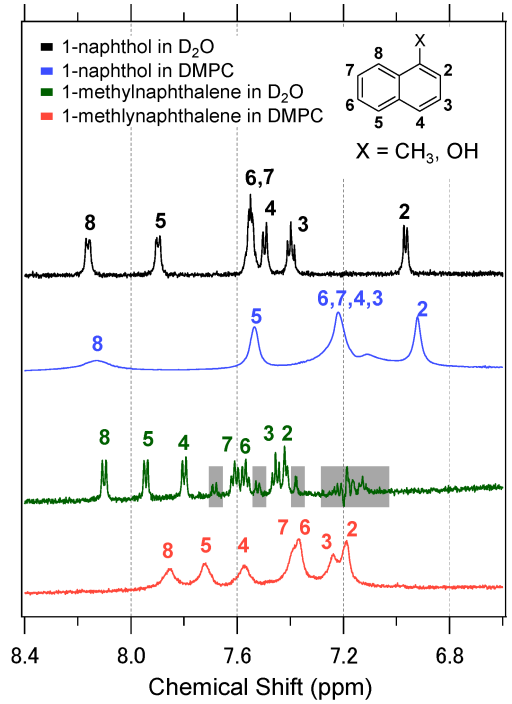

Figure 2. Ring proton regions in the ^{1}H-NMR spectra of 1-naphthol and 1-methylnaphthalene in D_2O solution and in DMPC vesicle. The gray squares stand for the signals from impurities and the probe-specific artifacts seen only when the concentration is very low; 1-methylnaphthalene dissolves into water at ~0.1 mM.

3.1 NOE observations

In our NOE measurements, PCγ and PC14 were chosen as the sites irradiated by the selective π pulse.[69] They are the terminal sites of the lipid and are useful to examine the location and orientation of small molecules in the membrane. The use of the transient NOE-SE method enabled quantitative analysis of signal intensities due to the suppression of the broad components, as described in a previous paper.[46] Additionally, the spin echo and the field gradient contributed to the improvement of the S/N of small signals due to the suppression of the strong signals from lipids and water. Figure 3 illustrates the difference spectra of the aromatic region measured by the transient NOE-SE method. NOE is clearly detected and is stronger for 1-naphthol than for 1-methylnaphthalene.

The NOE cross relaxation rate constants σ of the naphthalene derivatives in the DMPC bilayer are shown in Figure 4. According to eqs 10–13, the cross relaxation rate constant σ obtained from NOE experiment is determined by the internuclear distance r and the correlation time τ_c. For each naphthalene derivative, the σ value is an indicator of the close contact with the proton site of DMPC since τ_c is found in subsection 3.2 to depend weakly on the proton sites from MD simulation. As seen in Figure 4, the σ with the PCγ and PC14 irradiations are comparable in magnitude for each site in the naphthalene derivative. This shows that the naphthalene derivative comes close to both the hydrophobic core and the hydrophilic headgroup. It is of particular interest that the NOEs between 1-

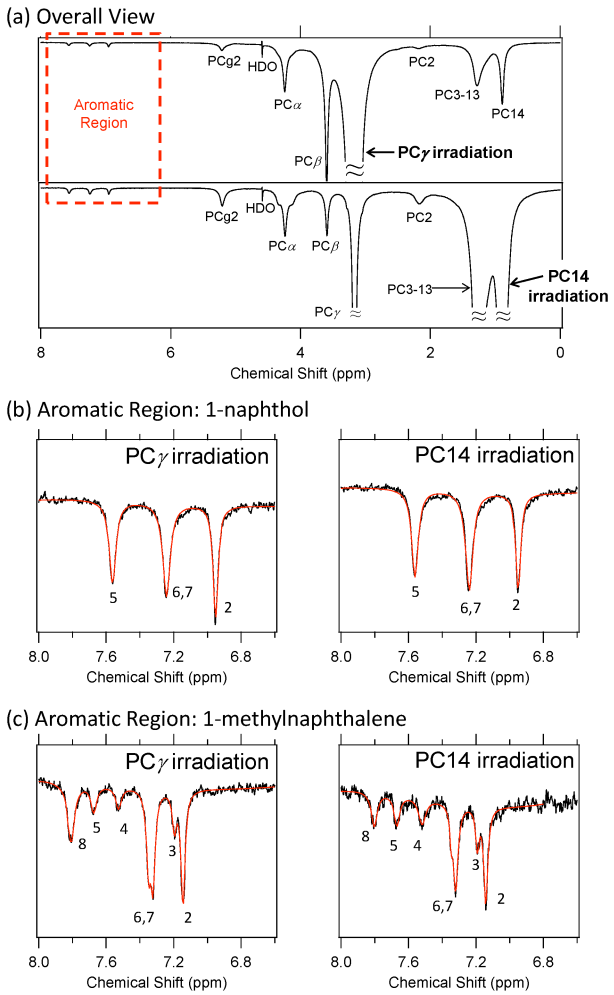

Figure 3. (a) The overall difference spectra for the 1-naphthol system. For 1-methylnaphthalene system, the overall difference spectra are observed similarly. (b) and (c) Difference spectra for the aromatic regions of the naphthalene derivatives due to the transient NOE-SE method. The H8 signal of 1-naphthol is not detected due to suppression by the spin-echo part of the transient NOE-SE method since it is a broad component. The peak at ~7.2 ppm for 1-naphthol is assigned to H67, but the possibility is not fully negated that H3 contributes to the peak. Thus, the peak at ~7.2 ppm is not subject to the quantitative analyses in the following. The red lines are the fits by a sum of Lorentz functions.

methylnaphthalene and PCγ are clearly observed. It indicates that the hydrophobic molecule even without hydrophilic group may stay close to the hydrophilic headgroup of lipid. An NOESY experiment was performed previously for benzene in SDS (sodium dodecyl sulfate) micelle, and the benzene distribution was found to be rather uniform in the SDS micellar interior.[44] The direct observation of close contact of small hydrophobic molecule with both the hydrophobic core and the hydrophilic headgroup of lipid is reported here for an essentially planar membrane at solution state, and is in agreement with MD results.[15,23] An interpretation of the wide distribution of hydrophobic solute in lipid membrane was given in ref 20. When the free energy of the solute's binding into membrane is decomposed into the lipid and water contributions, the lipid contribution is more favorable

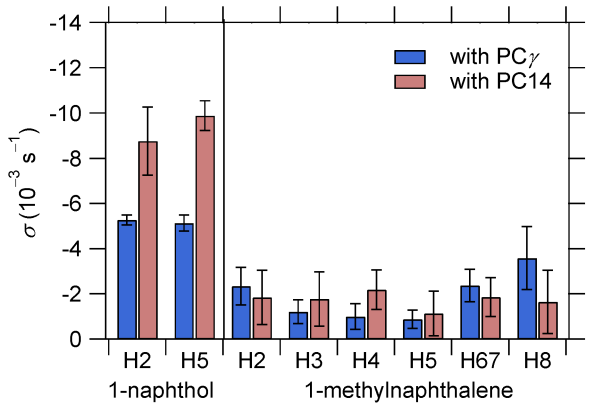

Figure 4. The cross relaxation rate constants σ between the naphthalene derivative and DMPC when the PCγ or PC14 is irradiated. The σ value on the ordinate decreases in the upward direction; this convention is adopted to highlight the magnitude (absolute value) of σ.

toward inner part of membrane. As far as the solute stays within the membrane and is not in the aqueous region, in contrast, water counteracts the lipid and its contribution is more favorable in outer domain of membrane. This is caused by the fact that the repulsive effect of water such as the excluded-volume effect reduces drastically in the membrane inside without substantial loss of dispersion attraction in the membrane-water interfacial domain. This role of water is not restricted to membrane-water interface, and a similar effect was observed at air-water interface and in low- to medium-density supercritical water[70, 71]

For each of PCγ and PC14, σ varies only weakly over the proton sites in the naphthalene derivative. This shows that the distance from either PCγ or PC14 is not sensitive to the sites in the naphthalene derivative. Thus, no specific orientation is inferred from the σ measurement. The orientation information will be further refined in subsection 3.2 in combination with MD simulation.

We next compare 1-naphthol and 1-methylnaphthalene. σ of 1-methylnaphthalene is smaller in magnitude than of 1-naphthol. The large absolute value of σ for 1-naphthol indicates that the correlation time τ_c of 1-naphthol is larger than of 1-methylnaphthalene, since the spatial distribution is similar between the two naphthalene derivatives. Though a quantitative analysis of the line width in DMPC bilayer is prevented by the overlapping of signals, Figure 2 shows that the line broadening of 1-naphthol is more evident than of 1-methylnaphthalene. This means the lower mobility of 1-naphthol in the bilayer, which is considered due to its hydrogen bonding ability.

3.2 Combination of MD and Experimental NOE

From MD simulation, we determined the time correlation function $C(t)$ introduced by eq 4. $C(t)$ is related to the cross relaxation rate constant σ through eq 3. In this subsection, we focus on the internuclear distance r and the correlation time τ_c defied by eq 5.

Figure 5 shows $C(t)$. The correlation functions $C(t)$ are well fit by a sum of three exponential functions in the form of eq 9. With this fit, τ_c is given by $\tau_c = \sum_{n=1}^{3} A_n \tau_n$ and is listed in Table 1. According to Figure 5, the $C(t)$ profile does not depend strongly

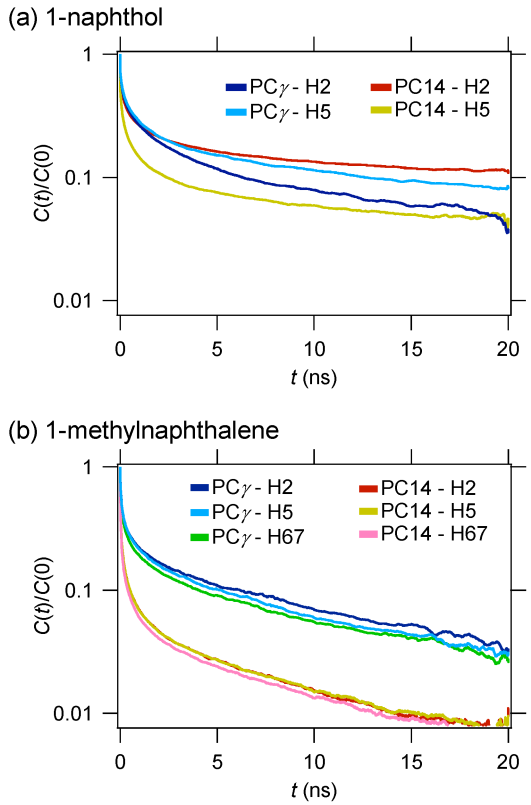

Figure 5. The normalized $C(t)$ between the terminals of lipid and the naphthalene derivative. The concentration of the naphthalene derivative is 40 mol%.

Table 1. Correlation times τ_c of eq 5 and $K(\omega_0)$ of eq 11 from MD.

^{1}H Assignment		τ_c (ns)		$K(\omega_0)$ (ns)	
		PCγ	PC14	PCγ	PC14
1-naphthol	H2	2.9	6.4	-2.7	-6.2
	H5	4.2	2.4	-4.0	-2.2
1-methylnaphthalene	H2	2.2	0.52	-2.0	-0.37
	H3	2.0	0.50	-1.8	-0.35
	H4	2.2	0.56	-2.0	-0.40
	H5	2.0	0.55	-1.8	-0.38
	H67	1.9	0.48	-1.6	-0.33
	H8	2.6	0.60	-2.4	-0.43

on the proton site of the naphthalene derivative when the irradiated site of DMPC is fixed at PCγ or PC14. Correspondingly, the τ_c value in Table 1 stays on the same order of magnitude over the proton site of small molecule. Although some of $C(t)$ does not decay within the timescale of Figure 5, the similarity of the decay profiles is evident. Note from eqs 10–13 that σ is proportional to r^{-6} and to τ_c. Even when τ_c is different by a factor of 3, for example, the same factor can be brought by a difference in r only by 20%. A difference of r causes a much larger change in σ than that of τ_c. Thus, the approximation of fixed τ_c is a good approximation unless τ_c varies over orders of magnitude. The internuclear correlation between lipid molecules themselves is a case of the order-of-magnitude variation of τ_c[46], and it is considered due to the lateral diffusion.[30, 72, 73] Table 1 shows that τ_c varies only by a factor of ~3 over the protons of the naphthalene derivatives. σ is then considered to mainly reflect the

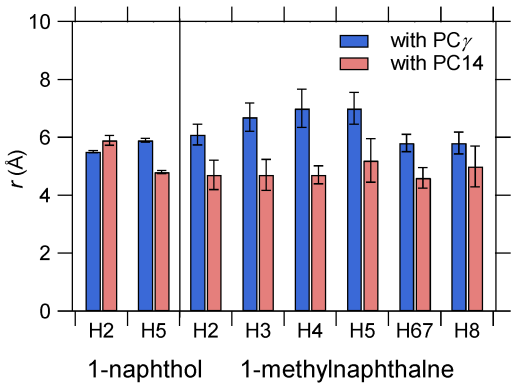

Figure 6. The distances r from PCγ and PC14 estimated by combining the experimental σ and the simulated τ_c. The error bar is estimated from the experimental σ, and does not reflect possible errors of τ_c from MD simulation.

distance information, and Table 1 validates the discussion of location and orientation described in subsection 3.1.

We next attempt to determine the "average" distance r between the naphthalene derivative and DMPC. To do so, we determine $K(\omega_0)$ of eq 11 from MD simulation (Table 1) and substitute it into eq 10 with the experimental σ. Since the dynamical information from MD is often semi-quantitative and some of $C(t)$ do not decay yet in Figure 5, our following discussion on r is also semi-quantitative and is justified within the allowance of τ_c described below. Still, our following discussion is valid even with the error in σ by a factor of 2.

Figure 6 shows the r thus estimated. r in Figure 6 is actually equal to $\langle r^{-6}\rangle^{-1/6}$ from eq 7, and is a statistical property determined from the probability distribution function of internuclear distance. The "average" distances from PCγ and PC14 are comparable for all the proton sites of both the naphthalene derivatives.[74] It is seen in Figure 6 that r of the proton in 1-methylnaphthalene is slightly smaller from PC14 than from PCγ. Figure 5 shows evidently that $C(t)$ with PCγ decays more slowly and enhances σ with PCγ. Even with comparable σ in Figure 4 between PCγ and PC14, the smaller r with PC14 is obtained in Figure 6 as far as τ_c is smaller with PC14 than with PCγ. Figure 6 shows that 1-methylnaphthalene prefers the hydrophobic domain slightly to the hydrophilic domain.

Finally, we discuss the orientation of small molecule in DMPC membrane from the dependence of r on the proton site of the naphthalene derivative in Figure 6. For 1-naphthol, H2 is more distant from PC14 than H5, showing a weak preference of the OH group toward the hydrophilic domain of membrane. It should be noted that dynamic properties of lipid membrane are not quantitative in MD simulation and that their MD values are typically different by factors of ~2 from experimental values.[17, 22] The r trend for 1-naphthol in Figure 6 is robust, though, since the order of r in Figure 6 is unchanged as far as the order of τ_c (to be exact, $K(\omega_0)$) stays invariant. The orientational preference is weak since the r variation is ~1 Å and the molecular size of the naphthalene derivative is ~5 Å. For 1-methylnaphthalene, there might seem a slight indication of the methyl group pointing outward. A definite conclusion cannot be drawn, however, for the orientational preference of 1-methylnaphthalene. Even with an error of τ_c by ~40%, the r trend of 1-methylnaphthalene reverses.

In Appendix C, we supplement our discussion on the interaction of the naphthalene derivative with lipid membrane by MD results.

4. Conclusions

The location, orientation, and dynamics of 1-naphthol and 1-methylnaphthalene in DMPC bilayer were investigated by solution-state ^{1}H-NMR. The transient NOE-SE method reported in a previous work[46] was employed to quantitatively observe the NOE between the small molecule and DMPC in large unilamellar vesicle in aqueous state. The NOE cross relaxation rate constant σ shows that both the naphthalene derivatives distribute over wide domain of membrane from the hydrophobic core to the hydrophilic headgroup. The close contacts of hydrophobic small molecule with both the hydrophobic core and the hydrophilic headgroup of lipid were directly observed in solution-state NOE, and are in agreement with previous MD results.[15,23] The mode of binding of the naphthalene derivative was further refined in combination with MD simulation. 1-Naphthol exhibits a weak orientational preference pointing its OH group toward the hydrophilic domain, while no definite conclusion was drawn for the orientation of 1-methylnaphthalene. The NOE rate constant σ was observed to be larger for 1-naphthol than for 1-methylnaphthalene. This reflects the slower motion of 1-naphthol, as evidenced in the signal broadening.

The naphthalene derivatives in this work are much smaller in size than the lipid forming the membrane. The time scales of their motions are rather uniform, and the NOE cross relaxation rate constant reflects mainly the distance information. When the lipid itself is examined by NOE, on the other hand, a previous work[46] showed that multiple scales are present in the lipid motion. The lipid size defines the thickness of (one leaflet of) the bilayer and the NOE between the lipids themselves is strongly affected by the dynamics. The dynamical influence on NOE is thus dependent on the molecular size, and it is of interest to address the interaction of lipid with a molecule of "intermediate" size.

Acknowledgements

This work is supported by the Grants-in-Aid for Scientific Research (Nos. 21300111 and 23651202) from the Japan Society for the Promotion of Science, by the Grant-in-Aid for Scientific Research on Innovative Areas (No. 20118002) from the Ministry of Education, Culture, Sports, Science, and Technology, and by the Nanoscience Program, the Computational Materials Science Initiative, and the Strategic Programs for Innovative Research of the Next-Generation Supercomputing Project.

Appendix A. Assignments of the ^{1}H signals and the Chemical Shifts

The signal assignments of the naphthalene derivatives in the DMPC system were conducted by comparison with the signals in *n*-octanol. The concentrations of the naphthalene derivatives were increased to 100 mM in *n*-octanol. The NMR measurements were performed by using JEOL ECA400 and ECA600 NMR spectrometers at 40 ºC. The DMPC small unilamellar vesicle (SUV) system containing 1-naphthol at 40 mol% was also measured. The SUV was prepared by ultrasonic irradiation of aqueous suspension of DMPC and 1-naphthol with MISONIX MICROSON Model XL2000 at an amplitude of 45 μm for 20 min.

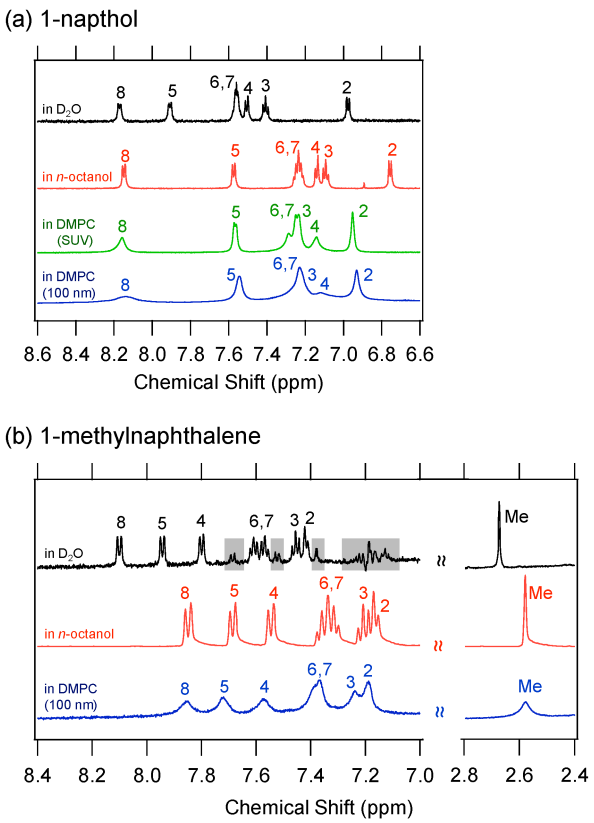

Figure A1. 1D spectra of (a) 1-naphthol and (b) 1-methylnaphthalene in D_2O, in *n*-octanol, and in DMPC membrane. The gray squares stand for the signals from impurities and the probe-specific artifacts seen only when the concentration is very low; 1-methylnaphthalene dissolves into water at ~0.1 mM. A break is present in the abscissa of (b). The ordinate scale is different in the left and right of the break.

Figure A1 demonstrates the ^{1}H signals of the naphthalene derivatives in D_2O, in *n*-octanol, and in DMPC membrane. The external reference for the chemical shift was dilute TMS in $CDCl_3$, and the spectra were corrected by the magnetic susceptibilities of water and *n*-octanol, respectively, for D_2O solution and DMPC system and for *n*-octanol solution. The signals in DMPC were assigned through comparison to those in *n*-octanol.

The ^{1}H signals of the naphthalene derivatives in *n*-octanol were assigned through COSY and NOESY. The mixing time for the NOESY experiment was 3 s. Figure A2 shows the COSY and NOESY spectra of 1-naphthol, and Figure A3 is for 1-methylnaphthalene. The 1D ^{1}H spectrum acquired separately is used as the projections of the 2D spectra. Most ^{1}H signals could be assigned from the integration values, the splittings, and the COSY spectra. The proton sites 5 and 8 of 1-naphthol and 1-methylnaphthalene were determined by the NOESY spectra.

We also show that the addition of the naphthalene derivative does not cause significant effects on DMPC signals. Figure A4 illustrates the DMPC signals of the pure DMPC membrane, DMPC with 1-naphthol, and DMPC with 1-methylnaphthalene. The effect of added naphthalene derivative is weak even at 40

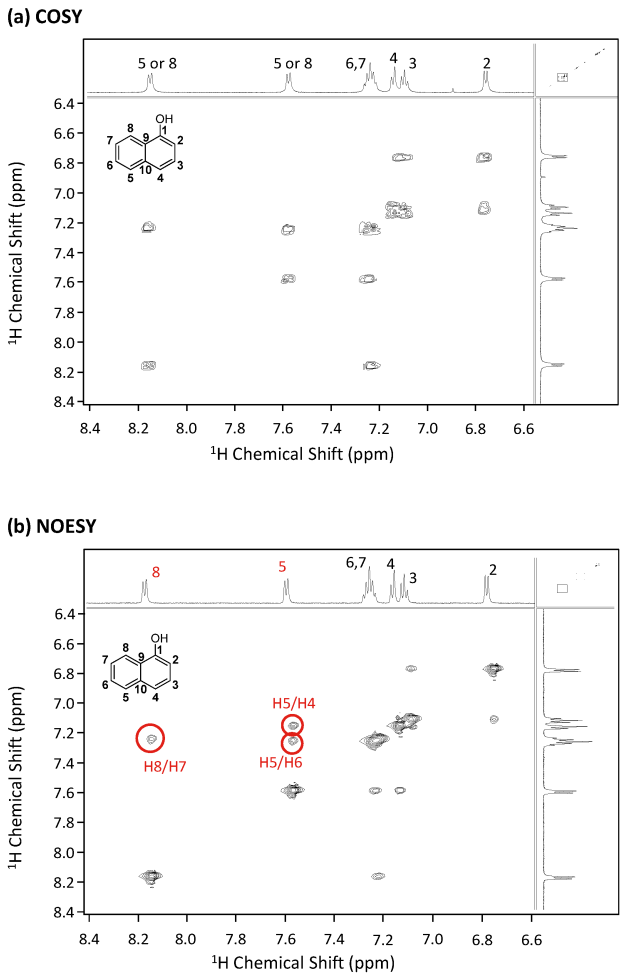

Figure A2. (a) The COSY and (b) NOESY spectra of 1-naphthol in *n*-octanol.

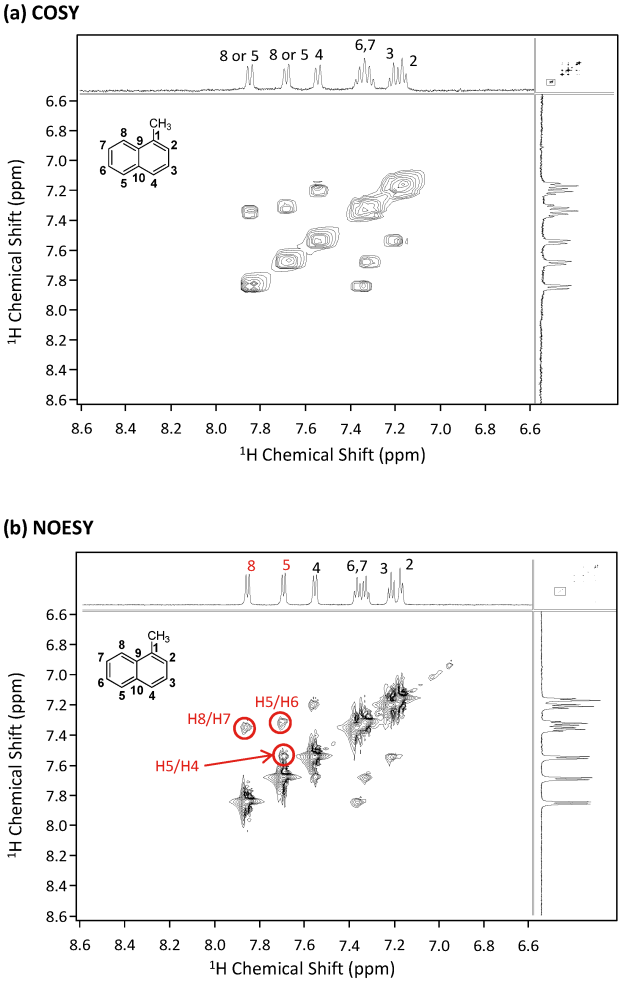

Figure A3. (a) The COSY and (b) NOESY spectra of 1-methylnaphthalene in *n*-octanol.

mol%. The changes in the line widths of the DMPC signals upon addition of the naphthalene derivative are smaller by orders of magnitude compared to the cases of larger molecules such as cholesterol.[8] The naphthalene derivative is small in size and the fluidity of membrane is not affected appreciably by its addition at 40 mol%.

We further examined the effect of addition of the naphthalene derivative on the phase transition of lipid membrane. It was reported by a differential scanning calorimetry study[75, 76] that aromatic compounds lower the phase transition temperature T_m. We measured ^{1}H-NMR spectra in the temperature range from 24 to 18 °C. The sharp ^{1}H-NMR signals of DMPC, which are indicative of the liquid-crystalline phase, were observed at 24 °C, and the changes in the line widths were virtually absent from 24 to 18 °C. This observation shows that T_m reduces by addition of the naphthalene derivative and that there is no transition from the liquid-crystalline phase to the gel phase even at 18 °C. In the present study, the NOE measurements and MD simulation were performed at 40 °C, which is well above T_m.

Table A1 shows the variations of the chemical shifts of the naphthalene derivatives upon binding into the lipid membrane. The chemical shifts move upfield (toward low-frequency region) in DMPC relative to those in D_2O. The upfield shift for 1-naphthol is less than 0.05 ppm for H2 and H8 and is ~0.3 ppm for the other sites. For 1-methylnaphthalene, all the sites exhibit a rather uniform upfield shift of ~0.25 ppm. The DMPC signals also shift upfield upon binding of the naphthalene derivative when compared to the pure DMPC vesicle. The upfield shift can be induced either by the contact of the naphthalene derivative with the electron-rich headgroup or by the reduction of deshieling effect on the ring protons by the hydrophobic chain of DMPC; the distinction is not evident for the effects from the hydrophilic and hydrophobic domains of lipid. Still, the observed trend of the chemical shifts is not inconsistent with the NOE results that 1-naphthol points its OH group toward the hydrophilic headgroup and that no obvious preference of location and orientation is present for 1-methylnaphthalene.

Appendix B. Mixing-Time Dependence

Figure A5 illustrates the dependence of the NOE enhancements η of 1-naphthol with PCγ on the mixing time τ_m at 50, 100, and 200 ms. η is monotonic at least up to τ_m = 200 ms. According to Figure A5, the initial rate approximation is of ~20% error; the discussion in the main text is not affected by this error.

Appendix C. Detailed MD Analysis

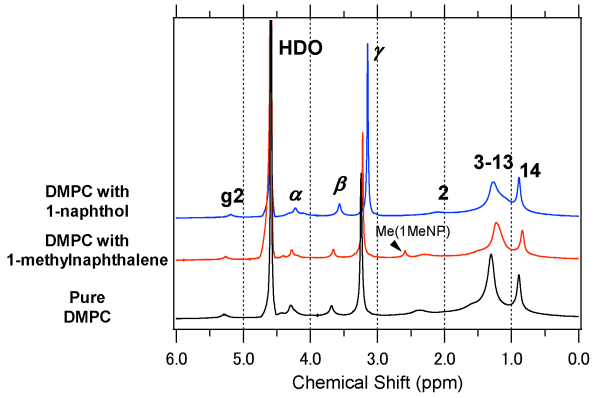

Figure A4. DMPC regions in the ^{1}H-NMR spectra of the membrane systems with and without naphthalene derivative.

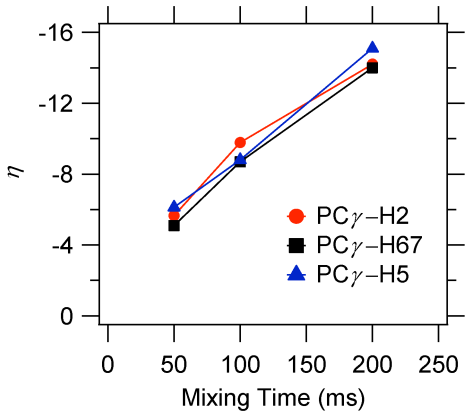

Figure A5. The mixing-time τ_m dependence of the NOE enhancement η.

We examine the concentration effect of the naphthalene derivative on its location and dynamics in the membrane. This is done to validate the experimental condition of the high concentration of the naphthalene derivative at 40 mol%. In Figures A6 and A7, the r and $C(t)$ of proton pairs of interest are plotted for the two systems of 40 mol% and 10 mol%. The r's are virtually the same between the 40 mol% and 10 mol% systems, and the $C(t)$'s of the two systems overlap well with each other. Thus, the concentration effect of the naphthalene derivative is not appreciable and our experimental setup for NMR measurement is validated.

The computed r in Figure A6 is in good agreement with the r in Figure 6 obtained from the combination of the experimental NOE σ and the computed τ_c. Figure A8 shows the proton distributions of the naphthalene derivatives and DMPC along the bilayer normal. Both the naphthalene derivatives distribute over wide domain from the hydrophobic core to the hydrophilic headgroup. For 1-naphthol, the distribution depends on the proton sites. H2 and OH distribute toward the hydrophilic side of bilayer, and H5 is close to the hydrophobic core. 1-Naphthol prefers to orient its OH group toward the hydrophilic portion. The distributions of all the protons in 1-methylnaphthalene are nearly identical, and no preferential orientation is detected.

Table A1. Chemical-shift variations $\Delta\delta$ of DMPC and the naphthalene derivatives upon binding.

^{1}H Assignment		$\Delta\delta$ (ppm) [a]	
		1-naphthol	1-methylnaphthalene
Naphthalene derivative	Me	-	-0.12
	H2	-0.03	-0.25
	H3	-0.31 [b]	-0.24
	H4	-0.31 [b]	-0.22
	H5	-0.34	-0.25
	H6	-0.31 [b]	-0.25
	H7	-0.31 [b]	-0.24
	H8	-0.01	-0.28
DMPC	PCγ	-0.08	-0.03
	PCβ	-0.10	-0.04
	PCα	-0.05	-0.02
	PCg2	-0.08	-0.03
	PC2	-0.21	-0.10
	PC3-13	-0.04	-0.11
	PC14	0.01	-0.05

[a] For DMPC, $\Delta\delta$ is defined as the difference of the chemical shift in the vesicle with the naphthalene derivative from that in the pure vesicle. For the naphthalene derivative, $\Delta\delta$ is defined as the difference of the chemical shift in the DMPC vesicle from that in D_2O. A negative value indicates an upfield shift relative to the pure DMPC vesicle or to the D_2O solution.
[b] The peaks overlap for H3, H4, H6, and H7 in the DMPC bilayer.

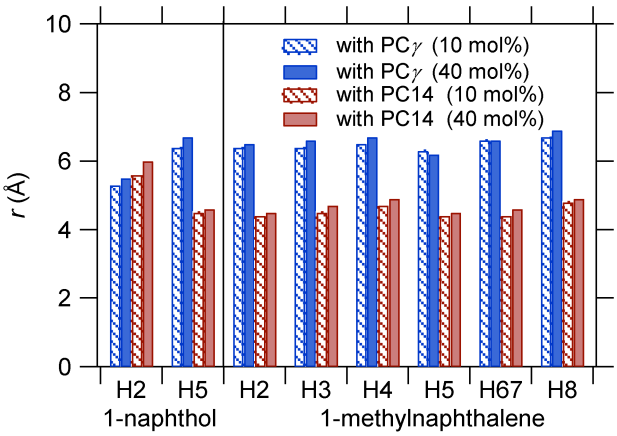

Figure A6. The calculated r for the 40 mol% and 10 mol% systems.

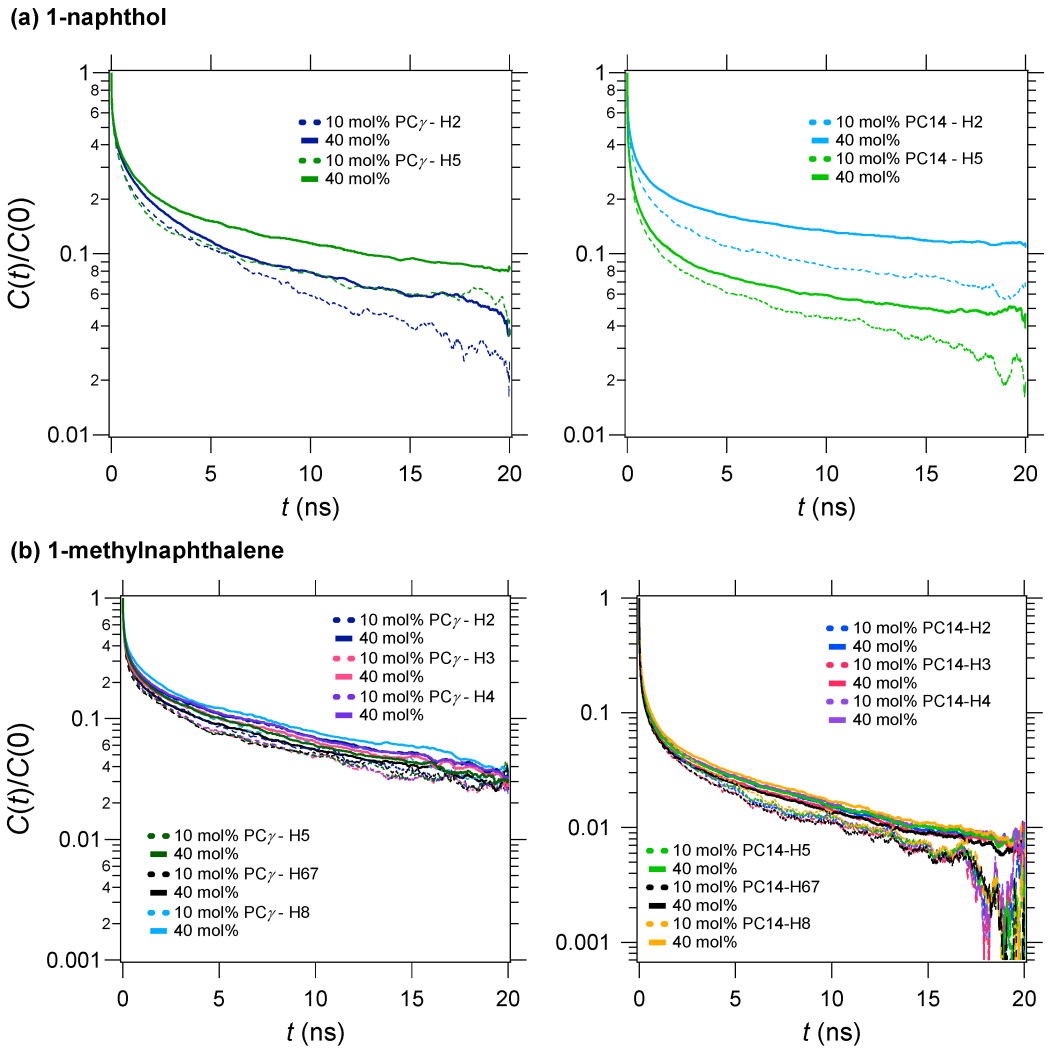

Figure A7. Comparison of the normalized $C(t)$ of (a) 1-naphthol and (b) 1-methylnaphthalene for the 40 mol% and 10 mol% systems.

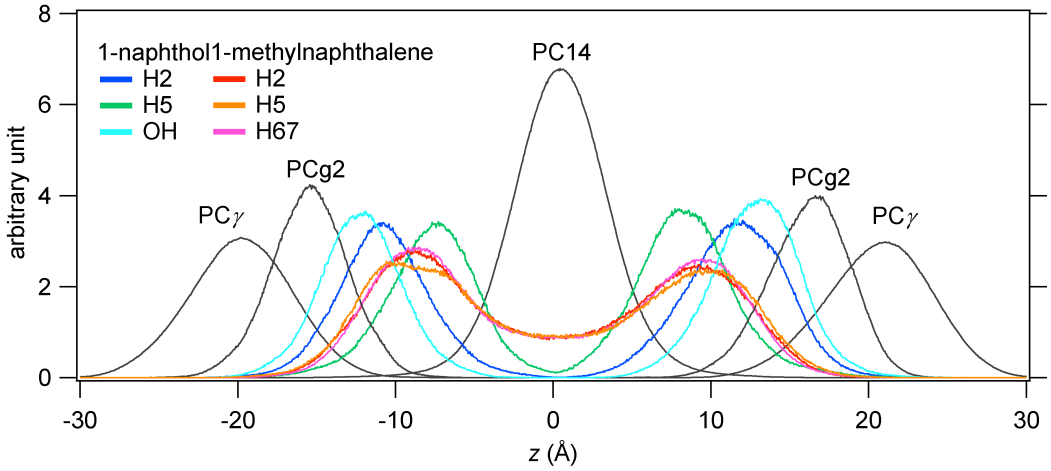

Figure A8. Proton distributions of the naphthalene derivatives and DMPC along the bilayer normal obtained from MD simulation. The center of the hydrophobic core is set to 0 Å.

References and Notes

1 A. M. Smondyrev and M. L. Berkowitz, *Biophys. J.*, 1999, **77**, 2075–2089.

2 M. Pasenkiewicz-Gierula, T. Róg, K. Kitamura and A. Kusumi, *Biophys. J.*, 2000, **78**, 1376–1389.

3 A. Léonard, C. Escrive, M. Laguerre, E. Pebay-Peyraula, W. Néri, T. Pott, J. Katsaras and E. J. Dufouc, *Langmuir*, 2001, **17**, 2019–2030.

4 G. W. Feigenson and J. T. Buboltz, *Biophys. J.*, 2001, **80**, 2775–2788.

5 W. Guo, V. Kurze, T. Huber, N. H. Afdhal, K. Beyer and J. A. Hamilton, *Biophys. J.*, 2002, **83**, 1465-1478.

6 H. A. Scheidt, D. Huster and K. Gawrisch, *Biophys. J.*, 2005, **89**, 2504–2512.

7 Z. Arsov and L. Quaroni, *Chem. Phys. Lipids*, 2007, **150**, 35–48.

8 C. Giordani, C. Wakai, K. Yoshida, E. Okamura, N. Matubayasi and M. Nakahara, *J. Phys. Chem. B*, 2008, **112**, 2622–2628.

9 T. Róg, M. Pasenkiewicz-Gierula, I. Vattulainen and M. Karttunen, *Biochim. Biophys. Acta*, 2009, **1788**, 97–121.

10 M. F. Roberts, A. G. Redfield and U. Mohanty, *Biophys. J.*, 2009, **97**, 132–141.

11 S. Marrink and H. J. C. Berendsen, *J. Phys. Chem.,* 1996, **100**, 16729–16738.

12 I. Z. Zubrzycki, Y. Xu, M. Madrid and P. Tang, *J. Chem. Phys.,* 2000, **112**, 3437–3441.

13 K. Gawrisch, H. C. Gaede, M. Mihailescu and S. H. White, *Eur. Biophys. J.*, 2007, **36**, 281–291.

14 H. A. Scheidt and D. Huster, *Acta. Pharmacol. Sin.*, 2008, **29**, 35–49.

15 S. E. Feller, C. A. Brown, D. T. Nizza and K. Gawrisch, *Biophys. J.*, 2002, **82**, 1396–1404.

16 D. Bemporad, C. Luttmann and J. W. Essex, *Biophys. J.*, 2004, **87**, 1–13.

17 M. C. Pitman, F. Suits, K. Gawrisch and S. E. Feller, *J. Chem. Phys.*, 2005, **122**, 244715.

18 K. E. Norman and H. Nymeyer, *Biophys. J.*, 2006, **91**, 2046–2054.

19 N. Matubayasi, K. K. Liang and M. Nakahara, *J. Chem. Phys.*, 2006, **124**, 154908.

20 N. Matubayasi, W. Shinoda and M. Nakahara, *J. Chem. Phys.*, 2008, **128**, 195107.

21 J. L. MacCallum, W. F. D. Bennett and D. P. Tieleman, *Biophys. J.*, 2008, **94**, 3393–3404.

22 P. S. Niemelä, M. T. Hyvönen and I. Vattulainen, *Biochim. Biophys. Acta*, 2009, **1788**, 122–135.

23 R. W. Tejwani, M. E. Davis, B. D. Anderson and T. R. Stouch, *J. Pharm. Sci.*, 2011, **100**, 2136–2146.

24 E. de Paula, S. S. Schreier, H. C. Jarrell and L. F. Fraceto, *Biophys. Chem.*, 2008, **132**, 47–54.

25 J. Atkinson, T. Harroun, S. R. Wassall, W. Stillwell and J. Katsaras, *Mol. Nutr. Food. Res.*, 2010, **54**, 641–651.

26 L. L. Holte and K. Gawrisch, *Biochemistry*, 1997, **36**, 4669–4674.

27 D. Huster, K. Arnold and K. Gawrisch, *Biochemistry*, 1998, **37**, 17299–17308.

28 W. –M. Yau, W. C. Wimley, K. Gawrisch and S. H. White, *Biochemistry*, 1998, **37**, 14713–14718.

29 D. Huster, K. Arnold and K. Gawrisch, *J. Phys. Chem. B*, 1999, **103**, 243–251.

30 K. Gawrisch, N. V. Eldho and I. V. Polozov, *Chem. Phys. Lipids*, 2002, **116**, 135–151.

31 H. C. Gaede and K. Gawrisch, *Biophys. J.*, 2003, **85**, 1734–1740.

32 H. A. Scheidt, A. Pampel, L. Nissler, R. Gebhardt and D. Huster, *Biochim. Biophys. Acta*, 2004, **1663**, 97–107.

33 H. C. Gaede, W. –M. Yau and K. Gawrisch, *J. Phys. Chem. B*, 2005, **109**, 13014–13023.

34 L. S. Vermeer, B. L. de Groot, V. Réat, A. Milon and J. Czaplicki, *Eur. Biophys. J.*, 2007, **36**, 919-931.

35 T. Kimura, K. Cheng, K. C. Rice and K. Gawrisch, *Biophys. J.*, 2009, **96**, 4916–4924.

36 C. Zuccaccia, G. Bellachioma, G. Cardaci and A. Macchioni, *J. Am. Chem. Soc.*, 2001, **123**, 11020–11028.

37 D. Ma, Z. Liu, L. Li, P. Tang and Y. Xu, *Biochemistry*, 2005, **44**, 8790–800.

38 V. A. Jarymowycz and M. Stone, *J. Chem. Rev.*, 2006, **106**, 1624–1671.

39 J. Cavanagh, W. J. Fairbrother, A. G. Palmer III, M. Rance and N. J. Skelton, *Protein NMR Spectroscopy: Principles and Practice*; Academic Press, New York, 2nd edn., 2006.

40 S. A. Simon, R. V. McDaniel and T. J. McIntosh, *J. Phys. Chem.*, 1982, **86**, 1449–1456.

41 R. E. Wasylishen, J. C. T. Kwak, Z. Gao, E. Verpoorte, B. MacDonald and R. M. Dickson, *Can. J. Chem.*, 1991, **69**, 822–833.

42 E. Okamura and M. Nakahara, *J. Phys. Chem.*, 1999, **17**, 3505–3509.

43 E. Okamura, R. Kakitsubo and M. Nakahara, *Langmuir*, 1999, **15**, 8332–8335.

44 B. E. Hawrylak and D. G. Marangoni, *Can. J. Chem.*, 1999, **77**, 1241–1244.

45 G. Da Costa, L. Mouret, C. Chevance, E. Le Rumeur and A. Bondon, *Eur. Biophys. J.*, 2007, **36**, 933–942.

46 M. Shintani, K. Yoshida, S. Sakuraba, M. Nakahara and N. Matubayasi, *J. Phys. Chem. B*, 2011, **115**, 9106–9115.

47 E. Okamura, C. Wakai, N. Matubayasi, Y. Sugiura and M. Nakahara, *Phys. Rev. Lett.,* 2004, **93**, 248101.

48 R. N. A. H. Lewis, N. Mak and R. N. McElhaney, *Biochemistry*, 1987, **26**, 6118–6126.

49 W. S. Price, *Concepts Magn. Reson.*, 1998, **10**, 197–237.

50 R. Brüschweiler and D. A. Case, *Prog. Nucl. Magn. Reson. Spectrosc.*, 1994, **26**, 27–58.

51 N. Foloppe and A. D. MacKerell Jr., *J. Comput. Chem.*, 2000, **21**, 86–104.

52 S. E. Feller and A. D. MacKerell Jr., *J. Phys. Chem. B*, 2000, **104**, 7510–7515.

53 J. B. Klauda, B. R. Brooks, A. D. MacKerell Jr., R. M. Venable and R. W. Pastor, *J. Phys. Chem. B*, 2005, **109**, 5300–5311.

54 J. B. Klauda, R. W. Pastor and B. R. Brooks, *J. Phys. Chem. B*, 2005, **109**, 15684–15686.

55 W. L. Jorgensen, J. Chandrasekhar, J. D. Madura, R. W. Impey and M. L. Klein, *J. Chem. Phys.*, 1983, **79**, 926–935.

56 *Computational Biochemistry and Biophysics*, eds. O. M.

Becker, A. D. MacKerell Jr., B. Roux, and M. Watanabe, Marcel Dekker, Inc., New York, 2001.

57 Although the charge setting described in the text is not typically recommended, we did so because our purpose is to examine only semi-quantitative aspects. In order to justify the adopted charge set of 1-naphthol, we performed ab initio MO calculations for phenol and 1-naphthol in vacuum and in PCM water at the MP2 theory and the aug-cc-pVTZ basis set using GAUSSIAN09 program.[66] The calculated charge on the hydroxyl oxygen of 1-naphthol was larger by 0.04 than of phenol. We then carried out two MD simulations of 1-naphthol in TIP3P water; one employs the potential parameters for 1-naphthol just as is in the main text, and the other modifies the charges on the O and H atoms of the hydroxyl group by +0.04 and −0.04, respectively, with keeping the other parameters unchanged. The time correlation functions of Legendre second rank were calculated for the H2-H5 and O-H vectors. The correlation times were computed through the fit to a sum of three exponential functions in the form of eq 9 and $\tau_c = \sum_{n=1}^{3} A_n \tau_n$. The τ_c values from the two simulations are 12.1 and 12.3 ps for H2-H5 and 8.5 and 8.6 ps for O-H, respectively. The charge set adopted for our MD is thus considered suitable within a precision of 2%. The MD simulations were performed over 50 ns using NAMD ver.2.7b2 with the following setups.[65] One 1-naphthol and 1000 TIP3P water molecules were located in a cubic cell of edge length of 31 Å. The ensemble adopted was the *NVT* and the temperature was controlled at 40 °C using Langevin dynamics with a damping coefficient of 5 ps^{-1}. The electrostatic interaction was handled by the particle-mesh Ewald (PME) method with a real-space cutoff of 12.0 Å, a spline order of 4, a relative tolerance of 10^{-6}, and the reciprocal-space mesh size of 32×32×32.[61] The equation of motion was integrated with the velocity Verlet algorithm at a time step of 2 fs.[64] The bond lengths involving hydrogen atom were fixed for 1-naphthol with SHAKE and the water molecule was kept rigid with SETTLE.[63]

58 G. J. Martyna, D. J. Tobias and M. L. Klein, *J. Chem. Phys.*, 1994, **101**, 4177–4189.

59 S. E. Feller, Y. Zhang, R. W. Pastor and B. R. Brooks, *J. Chem. Phys.,* 1995, **103**, 4613–4621.

60 J. F. Nagle and S. Tristram-Nagle, *Biochim. Biophys. Acta*, 2000, **1469**, 159–195.

61 U. Essmann, L. Perera, M. L. Berkowitz, T. Darden, H. Lee and L. G. Pedersen, *J. Chem. Phys.*, 1995, **103**, 8577–8593.

62 B. R. Brooks, R. E. Bruccoleri, B. D. Olafson, D. J. States, S. Swaminathan and M. Karplus, *J. Comp. Chem.*, 1983, **4**, 187–217.

63 S. Miyamoto and P. A. Kollman, *J. Comp. Chem.*, 1992, **13**, 952–962.

64 W. C. Swope, H. C. Andersen, P. H. Berens and K. R. Wilson, *J. Chem. Phys.*, 1982, **76**, 637–649.

65 J. C. Phillips, R. Braun, W. Wang, J. Gumbart, E. Tajkhorshid, E. Villa, C. Chipot, R. D. Skeel, L. Kale and K. Schulten, *J. Comp. Chem.*, 2005, **26**, 1781–1802.

66 M. J. Frisch, G. W. Trucks, H. B. Schlegel, G. E. Scuseria, M. A. Robb, J. R. Cheeseman, G. Scalmani, V. Barone, B. Mennucci, G. A. Petersson, H. Nakatsuji, M. Caricato, X. Li, H. P. Hratchian, A. F. Izmaylov, J. Bloino, G. Zheng, J. L. Sonnenberg, M. Hada, M. Ehara, K. Toyota, R. Fukuda, J. Hasegawa, M. Ishida, T. Nakajima, Y. Honda, O. Kitao, H. Nakai, T. Vreven, J. A. Montgomery Jr., J. E. Peralta, F. Ogliaro, M. Bearpark, J. J. Heyd, E. Brothers, K. N. Kudin, V. N. Staroverov, R. Kobayashi, J. Normand, K. Raghavachari, A. Rendell, J. C. Burant, S. S. Iyengar, J. Tomasi, M. Cossi, N. Rega, J. M. Millam, M. Klene, J. E. Knox, J. B. Cross, V. Bakken, C. Adamo, J. Jaramillo, R. Gomperts, R. E. Stratmann, O. Yazyev, A. J. Austin, R. Cammi, C. Pomelli, J. W. Ochterski, R. L. Martin, K. Morokuma, V. G. Zakrzewski, G. A. Voth, P. Salvador, J. J. Dannenberg, S. Dapprich, A. D. Daniels, O. Farkas, J. B. Foresman, J. V. Ortiz, J. Cioslowski and D. J. Fox, *GAUSSIAN 09, Revision A.02*, Gaussian, Inc.: Wallingford CT, 2009.

67 To examine the exchange of the naphthalene derivative between lipid bilayer and bulk water, we measured the 40 mM DMPC system containing 3.2 mM 1-naphthol (8 mol%). The signal width of 1-naphthol is unchanged from that in 40 mol% system. Furthermore, the signals of the naphthalene derivative in the DMPC system do not merge with the signals in D_2O. Thus, the exchange rate is slow and the signal broadening of naphthalene derivative is caused by the incorporation into the DMPC bilayer.

68 C. Hansch, A. Leo and D. Hoekman, *Exploring QSAR: Hydrophobic, Electronic, and Steric Constants*. Washington, DC, American Chemical Society, 1995.

69 The irradiation signals were almost unaffected by the spin-echo. See Figure 5 in ref 46.

70 R. Vácha, P. Slavíček, M. Mucha, B. J. Finlayson-Pitts and P. Jungwirth, *J. Phys. Chem. A*, 2004, **108**, 11573–11579.

71 N. Matubayasi and M. Nakahara, *J. Chem. Phys.*, 2005, **122**, 074509.

72 S. E. Feller, D. Huster and K. Gawrisch, *J. Am. Chem. Soc.*, 1999, **121**, 8963–8964.

73 Table 1 shows $K(\omega_0) \approx -\tau_c$. This means that the dynamics determining the present NOE is slow in the sense that τ_c is larger than $1/\omega_0$. It should be noted, though, that τ_c of Table 1 are comparable to those for proximate pairs of protons in lipid-lipid correlation reported in ref 46, while much slower dynamics was observed between distant proton pairs.

74 Although a major rule-of-thumb is that the NOE reflects the interaction within 5 Å, the cross relaxation can occur from protons with distances of more than 5 Å. As illustrated in Figure 8 of ref 46, $\rho(r)r^{-6}$ does not vanish in $r > 5$ Å and makes a non-zero contribution to σ. Since $\rho(r)r^{-6}$ is a fast-decaying function, an intermolecular NOE tends to be much smaller than an intramolecular one; σ in Figure 4 is smaller by an order of magnitude than the typical, intramolecular σ.[36]

75 M. K. Jain and N. M. Wu, *J. Membrane Biol.*, 1977, **34**, 157–201.

76 R. N. A. H. Lewis and R. N. McElhaney, in *The Structure of Biological Membranes,* ed. P. L. Yeagle, CRC Press, Boca Raton, FL, 2nd edn., 2005, Chapter 2.

